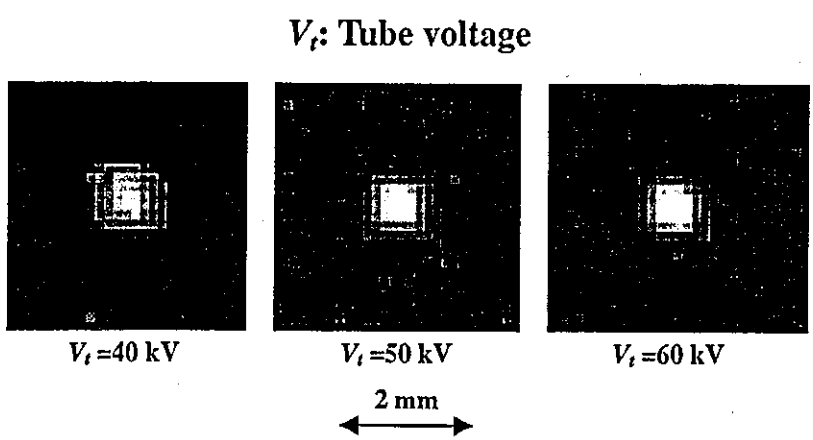

Fig. 3. Images of the X-ray source measured by a 100 mm diameter pinhole with changes in the tube voltage.

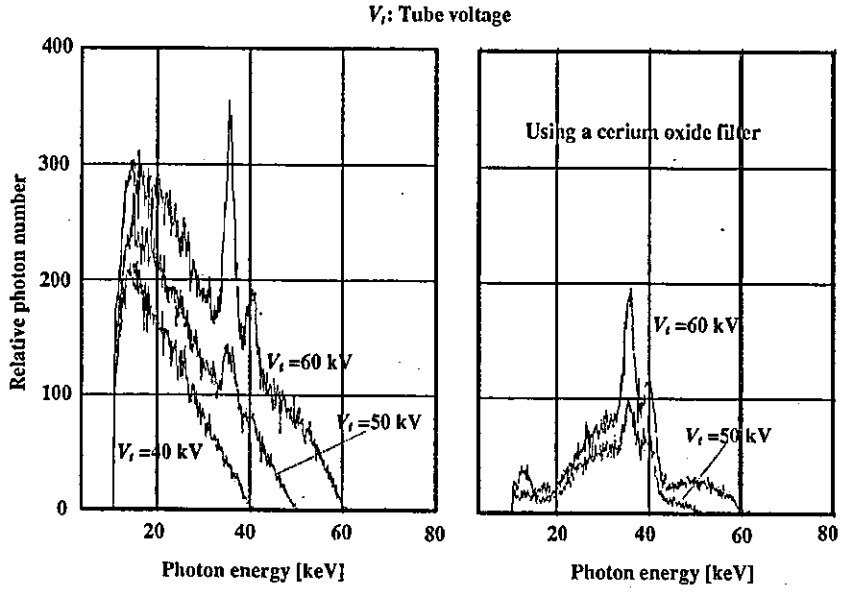

Fig. 4. X-ray spectra measured by a cadmium tellurium detector with changes in the tube voltage.

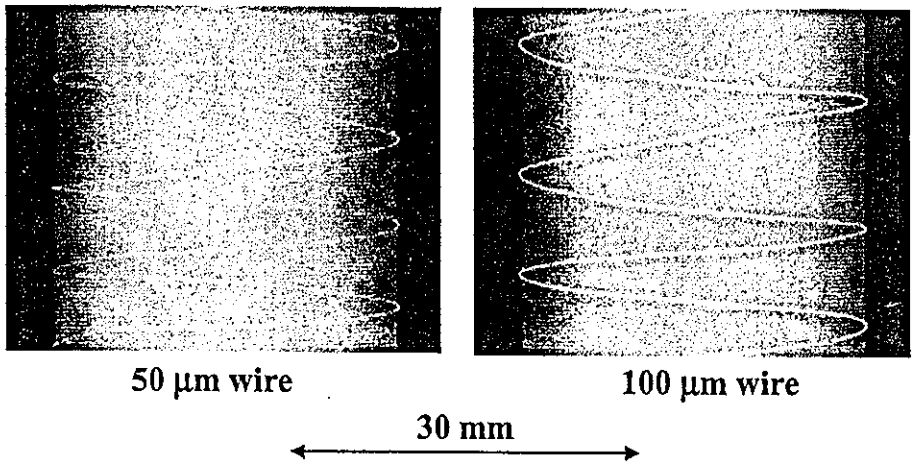

Fig. 5. Radiograms of tungsten wires around a rod made of PMMA used for estimating the image resolution.

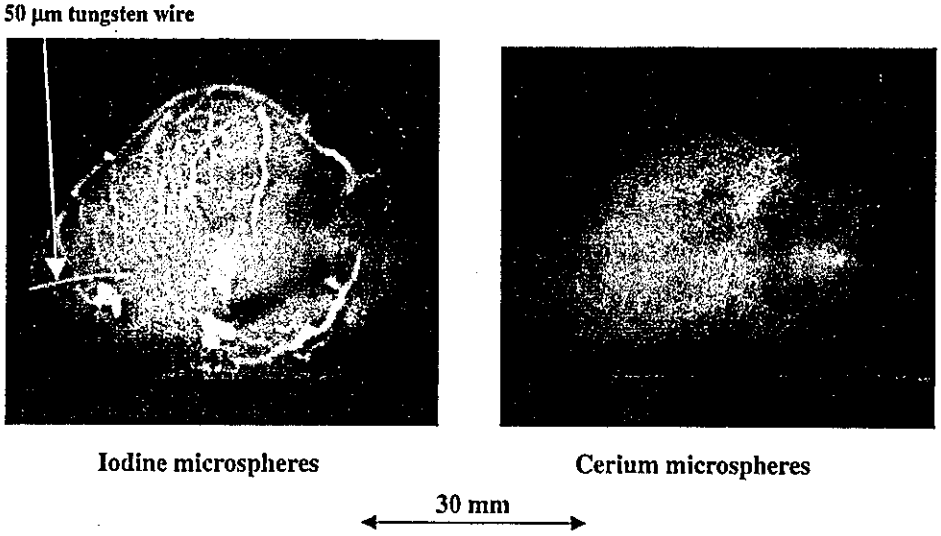

Fig. 6. Angiograms of rabbit hearts using (a) iodine and (b) cerium microspheres.

4. Angiography

The angiography was performed by a CR system (Konica Regius 150) using the monochromatic filter, and the distance (between the X-ray source and the imaging plate) and the tube voltage were 1.5 m and 60 kV, respectively.

Firstly, rough measurements of image resolution were made using wires. Fig. 5 shows radiograms of tungsten wires coiled around rods made of polymethyl methacrylate (PMMA). Although the image contrast increased with increases in the wire diameter, a 50 μm diameter wire could be observed.

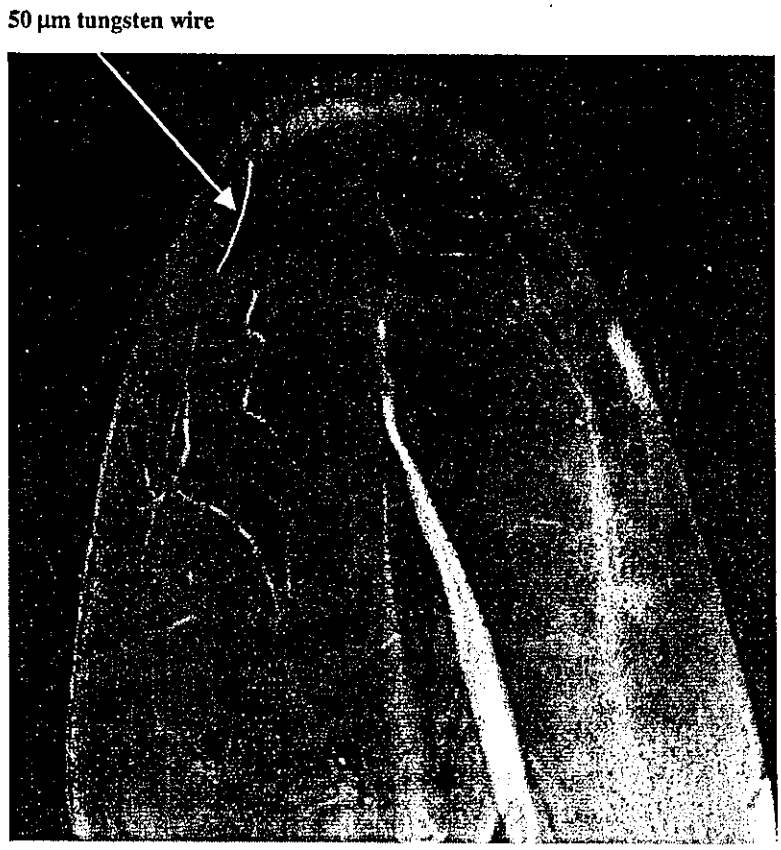

Fig. 7. Angiograms of the external ear of a rabbit using iodine-based microspheres. In this angiography, we employed a 50 μm tungsten wire to roughly determine the diameters of blood vessels.

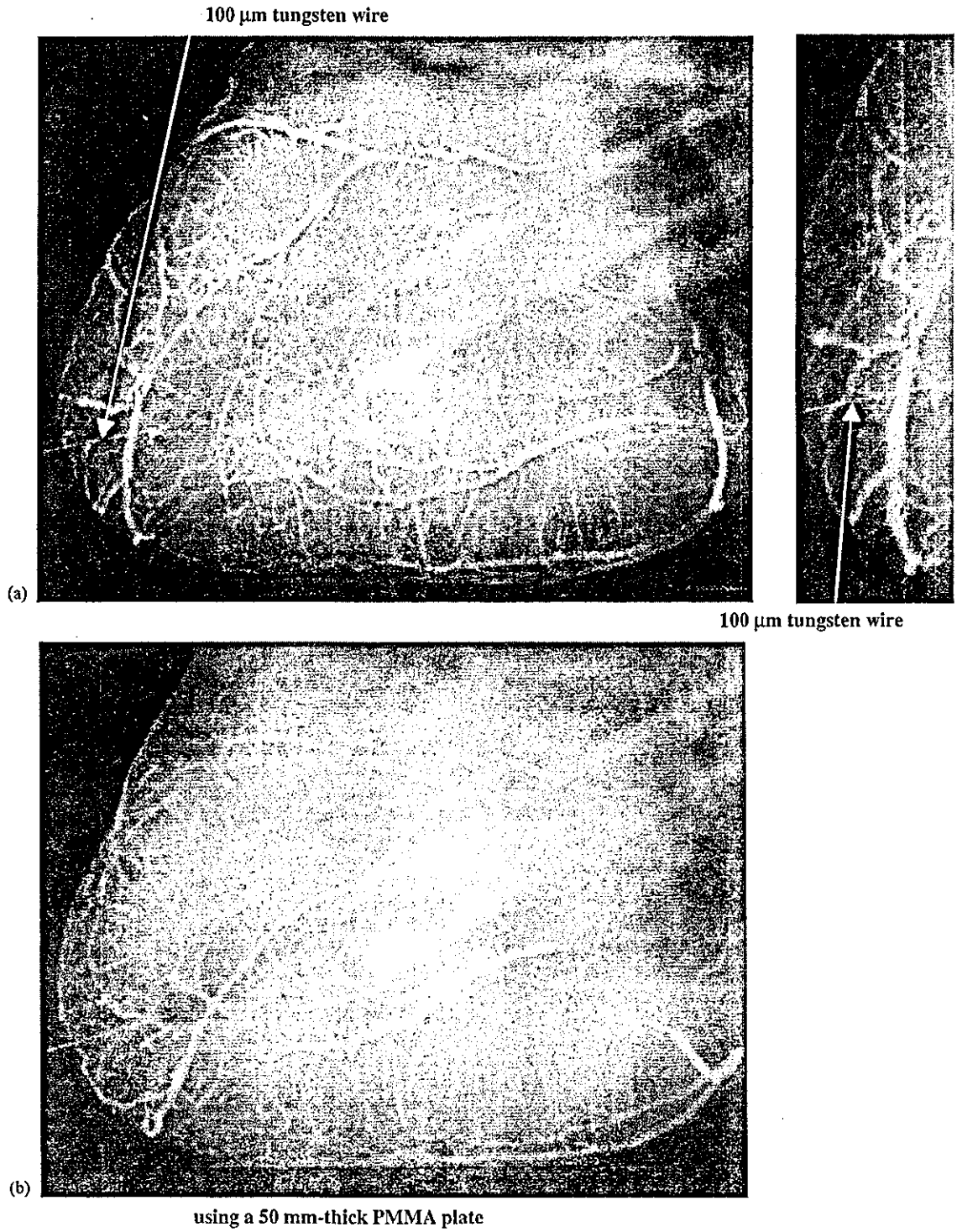

Fig. 8. Angiograms of an extracted heart of a dog. (a) Normal image and (b) image using a 50 mm PMMA plate set in front of the heart, facing the X-ray source.

Angiograms of rabbit hearts are shown in Fig. 6. These two images were obtained using iodine and cerium microspheres of 15 μm in diameter. In case where the cerium spheres were employed, the coronary arteries were barely visible. Fig. 7 shows an angiogram of the external ear of a rabbit using iodine spheres, and fine blood vessels of about 50 μm are clearly visible. In angiography of a larger heart extracted from a dog, using iodine spheres, a 50 mm thick PMMA plate was set in front of the heart facing X-ray source, and image contrast of coronary arteries decreased slightly with increases in the plate thickness (Fig. 8).

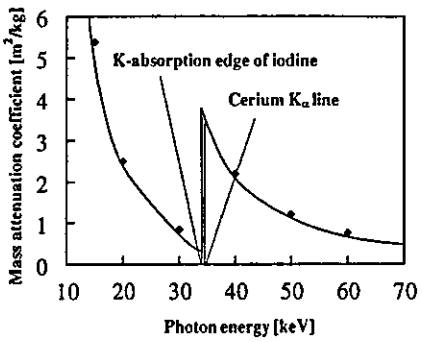

Fig. 9. Relation between the mass absorption coefficient of iodine and the photon energy of cerium Kα line.

5. Discussion

Cerium is a rare earth element and has a high reactivity. However, the average photon energy of Kα lines is 34.566 keV, and iodine spheres with a K-absorption edge of 33.155 keV absorb the lines easily (Fig. 9). Next, since the spheres easily transmit bremsstrahlung X-rays with energies of lower than the edge, it is important that the rays be absorbed as much as possible before angiography in order to increase the image contrast.

In rough measurement of image resolution, we obtained resolutions of 50 μm or less, and high-contrast blood vessels could be observed using a CR system. Although neogenetic fine blood vessels in recovery can be observed, the image resolution of the CR system should be improved as much as possible, and a dynamic CR system such as a flat panel system is useful to observe blood flows.

In this research, we developed a low-dose-rate X-ray tube in order to perform preliminary study on angiography using iodine-based contrast mediums. Because we are designing a high-dose-rate tube to decrease the exposure time, the K-series characteristic X-rays from cerium target can be employed to perform angiography for cases of cardiovascular disease.

6. Summary

In summary, we developed, new portable X-ray generator with a cerium-target tube and succeeded in producing K-series characteristic X-rays of cerium, which can be absorbed easily by iodine-based contrast mediums. Both the characteristic and bremsstrahlung X-ray intensities increased with corresponding increases in the tube voltage, and quasi-monochromatic X-rays were produced by a cerium oxide filter. In this preliminary experiment, although the maximum tube voltage and current were 65 kV and 0.4 mA, respectively, the voltage and current could be increased. Subsequently, we observed a 50 μm tungsten wire easily, and high-contrast angiography was performed using a CR system with an imaging plate.

Acknowledgements

This work was supported by Grants-in-Aid for Scientific Research and Advanced Medical Scientific Research from MECSST (12670902, 13470154, and 13877114), Grants from Keiryo Research Foundation, JST (Test of Fostering Potential), NEDO, and MHLW (HLSRG, RAMT-nano-001, RHGTEFB-genome-005, and RGCD13C-1).

References

[1] H. Mori, K. Hyodo, E. Tanaka, M.U. Mohammed, A. Yamakawa, Y. Shinozaki, H. Nakazawa, Y. Tanaka, T. Sekka, Y. Iwata, S. Honda, K. Umetani, H. Ueki, T. Yokoyama, K. Tanioka, M. Kubota, H. Hosaka, N. Ishizawa, M. Ando, Radiology 201 (1996) 173.
[2] T.J. Davis, D. Gao, T.E. Gureyev, A.W. Stevenson, S.W. Wilkims, Nature 373 (1995) 595.
[3] A. Momose, T. Takeda, Y. Itai, K. Hirano, Nature Med. 2 (4) (1996) 473.
[4] A. Ishisaka, H. Ohara, C. Honda, Opt. Rev. 7 (2000) 566.
[5] A. Mattsson, Phys. Scripta 5 (1972) 99.
[6] R. Germer, J. Phys. E Sci. Instrum. 12 (1979) 336.
[7] E. Sato, S. Kimura, S. Kawasaki, H. Isobe, K. Takahashi, Y. Tamakawa, T. Yanagisawa, Rev. Sci. Instrum. 61 (1990) 2343.
[8] E. Sato, M. Sagae, K. Takahashi, A. Shikoda, T. Oizumi, H. Ojima, K. Takayama, Y. Tamakawa, T. Yanagisawa, A. Fujiwara, K. Mitoya, SPIE 2513 (1994) 723.
[9] A. Shikoda, E. Sato, M. Sagae, T. Oizumi, Y. Tamakawa, T. Yanagisawa, Rev. Sci. Instrum. 65 (1994) 850.
[10] E. Sato, K. Takahashi, M. Sagae, S. Kimura, T. Oizumi, Y. Hayasi, Y. Tamakawa, T. Yanagisawa, Med. Biol. Eng. Comput. 32 (1994) 289.
[11] K. Takahashi, E. Sato, M. Sagae, T. Oizumi, Y. Tamakawa, T. Yanagisawa, Jpn. J. Appl. Phys. 33 (1994) 4146.
[12] E. Sato, M. Sagae, A. Shikoda, K. Takahashi, T. Oizumi, M. Yamamoto, A. Takabe, K. Sakamaki, Y. Hayasi, H. Ojima, K. Takayama, Y. Tamakawa, SPIE 2869 (1996) 937.
[13] E. Sato, Y. Hayasi, E. Tanaka, H. Mori, T. Kawai, T. Usuki, K. Sato, H. Obara, T. Ichimaru, K. Takayama, H. Ido, Y. Tamakawa, SPIE 4682 (2002) 538.
[14] E. Sato, R. Germer, Y. Hayasi, E. Tanaka, H. Mori, T. Kawai, T. Usuki, K. Sato, H. Obara, M. Zuguchi, T. Ichimaru, H. Ojima, K. Takayama, H. Ido, SPIE 4948 (2002) 604.
[15] E. Sato, Y. Hayasi, R. Germer, E. Tanaka, H. Mori, T. Kawai, H. Obara, T. Ichimaru, K. Takayama, H. Ido, Jpn. J. Med. Imag. Inform. Sci. 20 (2003) 148.
[16] E. Sato, Y. Hayasi, R. Germer, E. Tanaka, H. Mori, T. Kawai, H. Obara, T. Ichimaru, K. Takayama, H. Ido, Jpn. J. Med. Phys. 20 (2003) 123.
[17] E. Sato, K. Sato, Y. Tamakawa, Ann. Rep. Iwate Med. Univ. Sch. Lib. Arts Sci. 35 (2000) 13.

Available online at www.sciencedirect.com
SCIENCE DIRECT
JOURNAL OF ELECTRON SPECTROSCOPY and Related Phenomena
ELSEVIER
Journal of Electron Spectroscopy and Related Phenomena 137–140 (2004) 705–711
www.elsevier.com/locate/elspec

Quasi-monochromatic parallel radiography utilizing a computed radiography system

E. Sato[a,*], Y. Hayasi[a], R. Germer[b], E. Tanaka[c], H. Mori[d], T. Kawai[e], T. Ichimaru[f], S. Sato[g], K. Takayama[h], H. Ido[i]

[a] *Department of Physics, Iwate Medical University, Morioka 020-0015, Japan*
[b] *ITP, FHTW FB1 and TU-Berlin, D 12249 Berlin, Germany*
[c] *Department of Nutritional Science, Faculty of Applied Bio-science, Tokyo University of Agriculture, Setagayaku 156-8502, Japan*
[d] *Department of Cardiac Physiology, National Cardiovascular Center Research Institute, Osaka 565-8565, Japan*
[e] *Electron Tube Division #2, Hamamatsu Photonics Inc., Iwata-gun 438-0193, Japan*
[f] *Department of Radiological Technology, School of Health Sciences, Hirosaki University, Hirosaki 036-8564, Japan*
[g] *Department of Microbiology, School of Medicine, Iwate Medical University, Morioka 020-8505, Japan*
[h] *Shock Wave Research Center, Institute of Fluid Science, Tohoku University, Sendai 980-8577, Japan*
[i] *Department of Applied Physics and Informatics, Faculty of Engineering, Tohoku Gakuin University, Tagajo 985-8537, Japan*

Available online 21 March 2004

Abstract

A fundamental study on quasi-monochromatic parallel radiography using a polycapillary plate and a copper-target X-ray tube is described. The X-ray generator consists of a negative high-voltage power supply, a filament (hot cathode) power supply, and an X-ray tube. The negative high-voltage is applied to the cathode electrode, and the anode electrode is connected to the ground. In this experiment, the tube voltage was regulated from12–25 kV, and the tube current was regulated within 3.0 mA by the filament temperature. The exposure time was controlled in order to obtain optimum X-ray intensity, and the maximum focal spot dimensions were approximately 2 mm × 1.5 mm. The polycapillary plate was J5022-21 (Hamamatsu Photonics Inc.), and the plate thickness was 1.0 mm. The outer, effective, and hole diameters were 87 mm, 77 mm, and 25 μm, respectively. Quasi-monochromatic X-rays were produced using a 10 μm-thick copper filter, and these rays were formed into parallel beams by the polycapillary, and the radiogram was taken using a computed radiography system utilizing imaging plates. In the measurement of image resolution, the resolution fell according to increases in the distance between the chart and imaging plate using a polycapillary. We could observe a 50 μm tungsten wire clearly, and fine blood vessels of approximately 100 μm were visible in angiography.

Keywords: Parallel radiography; Quasi-monochromatic X-ray; Characteristic X-ray; X-ray lens; Polycapillary plate

1. Introduction

Thus far, we have developed several different soft flash X-ray generators [1–8] in order to perform soft radiographies with biomedical applications. In particular, plasma flash X-ray generators [9–11] are very useful to produce fairly high-dose-rate monochromatic X-rays as compared with a synchrotron. When a weakly ionized linear plasma formed using a rod target evaporation, irradiation of quite intense and sharp characteristic X-rays from the plasma axial direction was confirmed.

Monochromatic parallel radiography using synchrotrons plays important roles in microangiography [12] and X-ray phase imaging, [13–15] and further applications have long been wished for. In view of this situation, several different X-ray lenses have been developed [16,17], and a polycapillary plate [18–20] has been shown to be useful to realize a low-priced X-ray system and to perform parallel radiography. Therefore, we performed parallel radiography using a tungsten-target X-ray tube [19] and an X-ray film, and an image resolution of approximately 50 μm or less was obtained.

The tungsten target produced L-series characteristic and bremsstrahlung X-rays with tube voltages of 20–30 kV, and these rays were formed into parallel beams to perform radiography. Thereafter, K-series characteristic X-rays could

* Corresponding author.
E-mail address: dresato@iwate-med.ac.jp (E. Sato).

0368-2048/$ – see front matter © 2004 Elsevier B.V. All rights reserved.
doi:10.1016/j.elspec.2004.02.008

be employed for quasi-monochromatic and monochromatic radiographies using filters. In these cases, the photon energies of characteristic X-rays were determined by the target element.

In this research, we performed preliminary study on quasi-monochromatic parallel radiography utilizing a polycapillary plate, a Computed Radiography (CR) system [21], and a copper-target radiation tube in order to create a new X-ray system to be used instead of the synchrotron.

2. Experimental set-up

Fig. 1 shows the circuit diagram of the X-ray generator, which consists of a negative high-voltage power supply, a filament (hot cathode) power supply, and a copper-target X-ray tube. The negative high-voltage is applied to the cathode electrode, and the anode (target) is connected to the ground. In this experiment, the tube voltage was regulated from 15–25 kV, and the tube current was regulated by the filament temperature and ranged from 1.0–3.0 mA. The exposure time was controlled in order to obtain optimum X-ray intensity.

The experimental set-up for performing parallel radiography is shown in Fig. 2. Quasi-monochromatic X-rays are produced using a 10 μm-thick copper filter, and these rays are formed into parallel beams by a polycapillary plate. The polycapillary is J5022-21 (Hamamatsu Photonics Inc.), and the thickness and the hole diameter of the polycapillary are

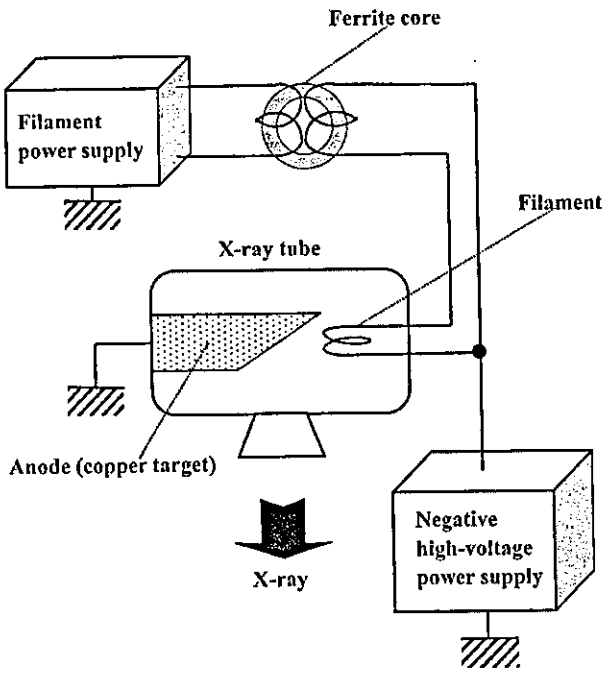

Fig. 1. Circuit diagram of the X-ray generator. Because the negative high voltage is applied to the cathode electrode, the tube voltage is −1 times the cathode voltage. The X-ray tube employs a 0.5 mm-thick beryllium window in order to produce soft X-rays effectively.

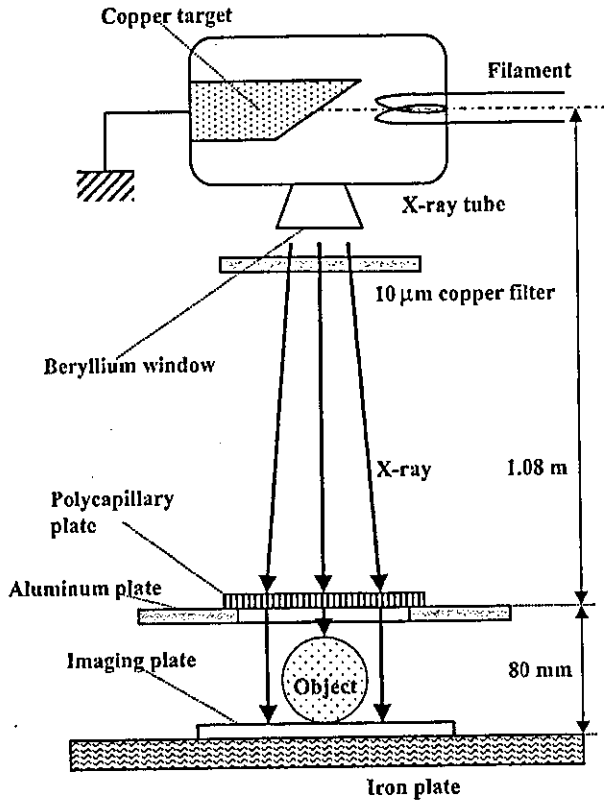

Fig. 2. Experimental set-up for parallel radiography utilizing a polycapillary plate and a CR system. Quasi-monochromatic X-rays are formed into parallel beam by a polycapillary, and the image is taken by a CR system.

1.0 mm and 25 μm, respectively (Fig. 3). Radiography was performed by a CR system (Konica Regius 150) utilizing imaging plates.

The distance between the X-ray source and the polycapillary was 1.08 m, and the polycapillary plate was placed on the aluminum plate, and the distance between the aluminum and imaging plates was regulated by the height of polymethyl methacrylate (PMMA) spacers of 30 mm in height.

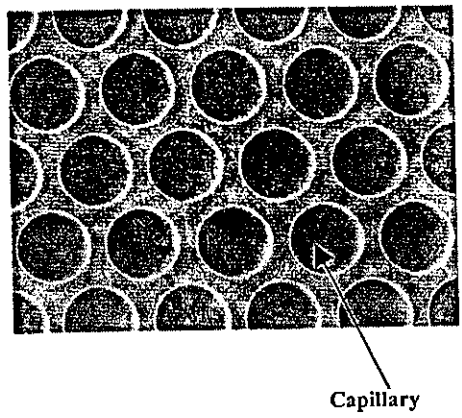

Fig. 3. Magnification of a polycapillary plate with a thickness of 1.0 mm and a hole diameter of 25 μm, respectively.

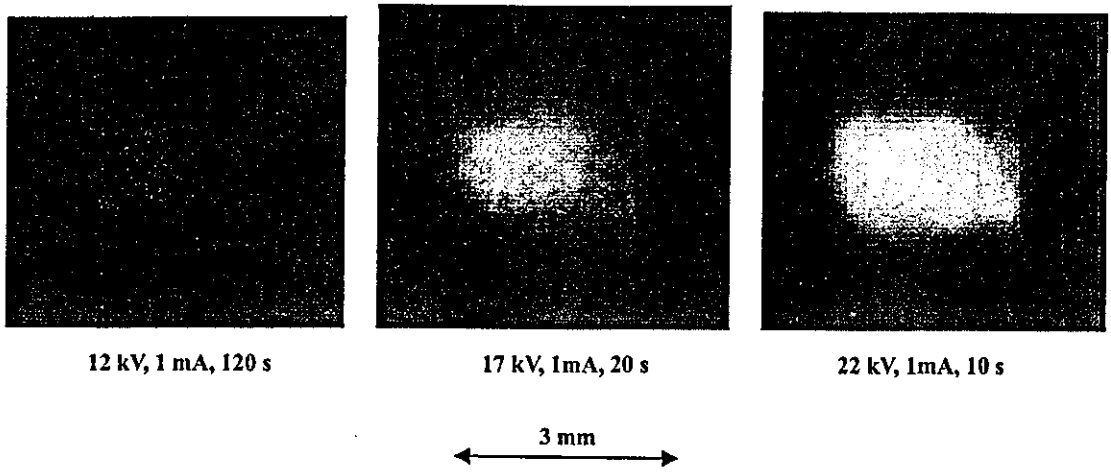

Fig. 4. Images of the X-ray source measured by a 50 μm-diameter pinhole with changes in the tube voltage.

3. Characteristics

3.1. Focal spot

In order to measure images of the X-ray source, we employed a pinhole camera with a hole diameter of 50 μm (Fig. 4). When the tube voltage was increased, the spot intensity increased, and spot dimensions increased slightly and had values of approximately 2 mm × 1.5 mm.

3.2. X-ray spectra

X-ray spectra from the copper-target tube were measured by a transmission-type spectrometer (Fig. 5) with a lithium fluoride curved crystal 0.5 mm in thickness. The spectra were taken by the CR system with a wide dynamic range, and relative X-ray intensity was calculated from Dicom digital data. Fig. 6 shows measured spectra from the copper target. When the tube voltage was increased, the bremsstrahlung X-ray intensity increased, and the characteristic X-ray intensity of K_α and K_β lines also increased. Following insertion of the copper filter, since the bremsstrahlung X-rays with energies higher than the K-absorption edge were absorbed effectively, we observed the edge.

4. Radiography

The quasi-monochromatic radiography was performed with a tube voltage of 20 kV using the filter. Fig. 7 shows radiography for imaging a polycapillary plate, and the radiograms of the polycapillary are shown in Fig. 8. The center of the black spot in the polycapillary radiogram was mainly imaged by direct transmission beams through capillary holes. As shown in this figure, both the spot density and the dimensions hardly varied according to decreases in the polymethyl methacrylate (PMMA) spacer height.

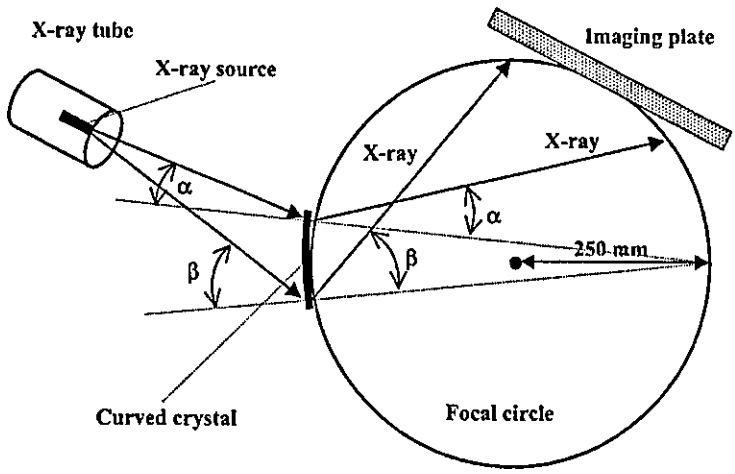

Fig. 5. Transmission-type spectrometer with a lithium fluoride curved crystal and an imaging plate. The X-rays from the source are diffracted by the crystal and are imaged on the imaging plate.

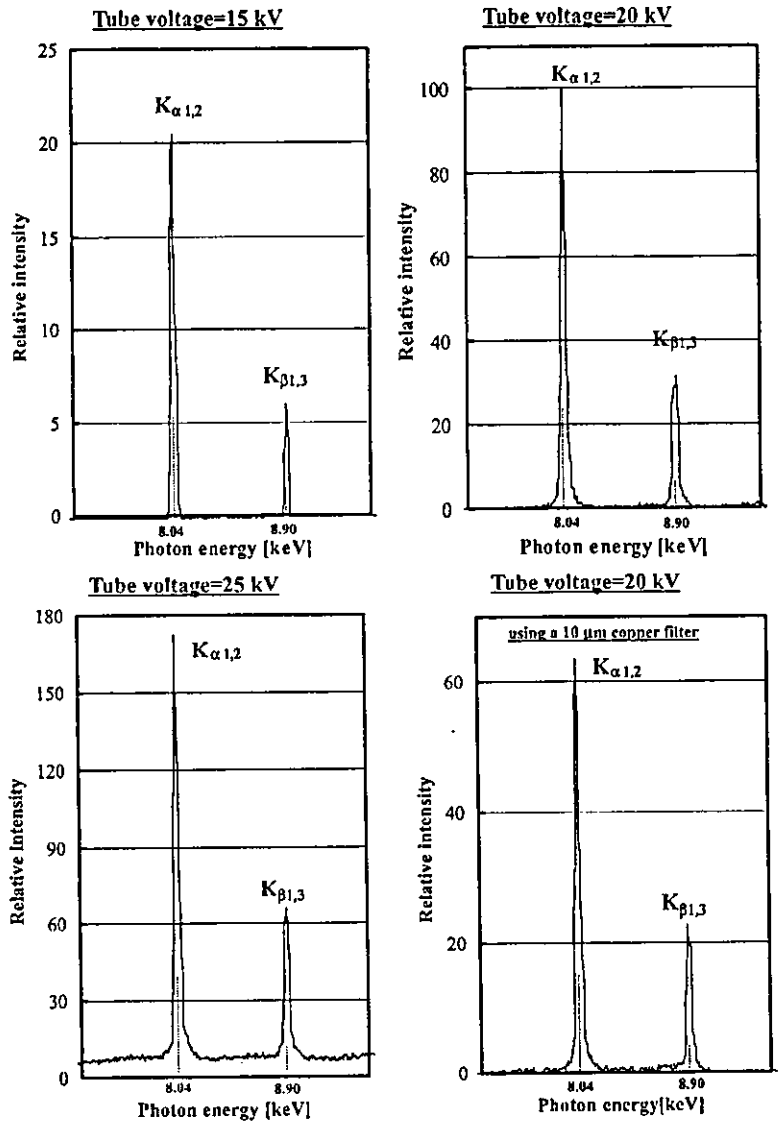

Fig. 6. Measured X-ray spectra according to changes in the tube voltage. Both the bremsstrahlung and characteristic X-ray intensities increased with corresponding increases in the tube voltage, and we determined the conditions for radiography as follows: a tube voltage of 20 kV and a filter thickness of 10 μm.

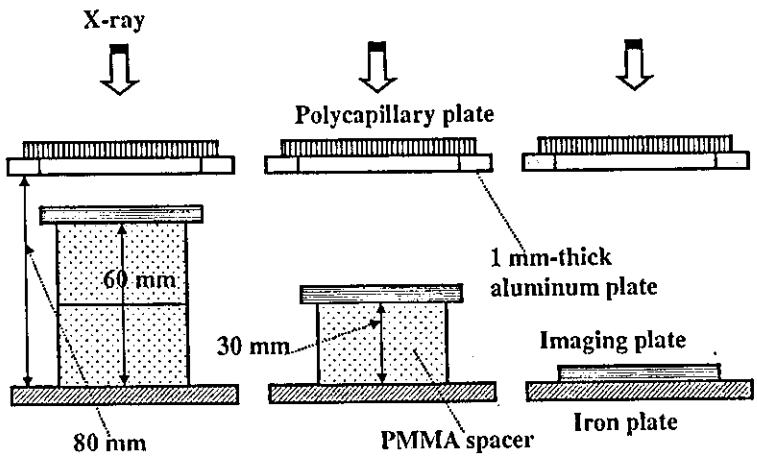

Fig. 7. Radiography for imaging a polycapillary plate according to changes in the distance between the polycapillary and imaging plates. Because the distance was regulated by the spacer thickness, the distance decreased according to increases in the spacer height.

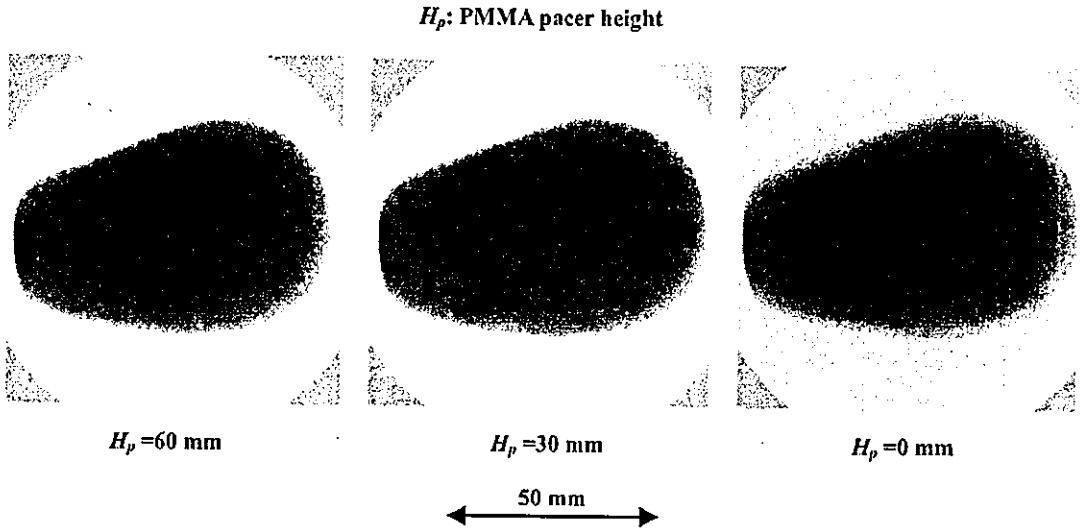

Fig. 8. Radiograms of a polycapillary plate according to changes in the PMMA height.

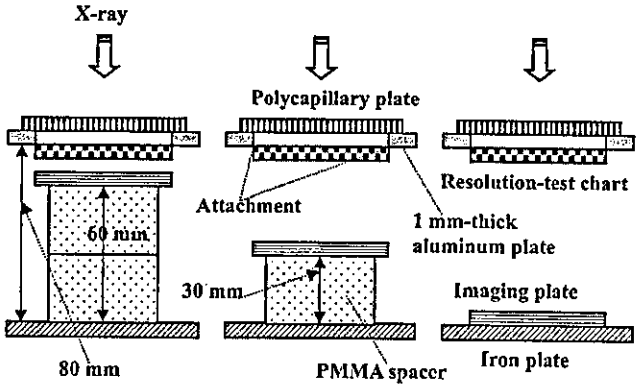

Fig. 9. Radiography for imaging a test chart using a polycapillary plate.

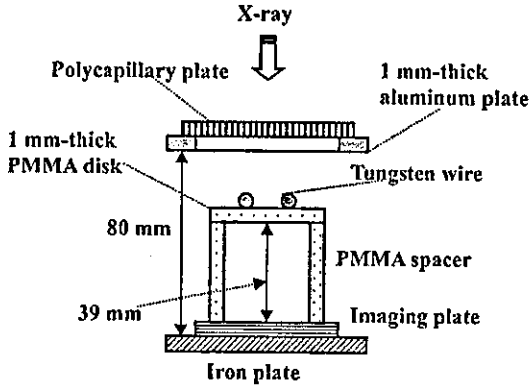

Fig. 11. Radiography for imaging tungsten wires using the polycapillary.

Fig. 9 shows the parallel radiography for imaging a test chart, and the polycapillary was placed on the aluminum plate. In this radiography, when the spacer height was increased, we observed 100 μm lines, and the image dimensions decreased slightly (Fig. 10).

Figs. 11 and 12 show radiography and the radiogram of tungsten wires on a PMMA spacer, respectively. Although the image contrast increased with increases in the wire diameter, a 50 μm-diameter wire could be observed. An angiography of a rabbit heart is shown in Fig. 13; iodine-based

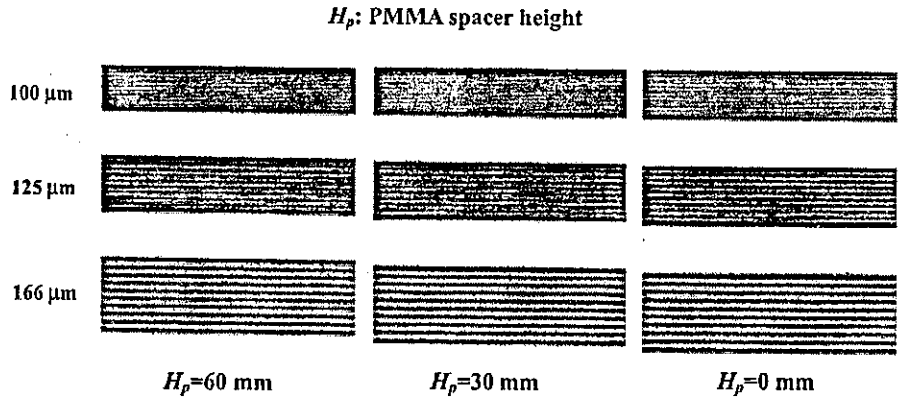

Fig. 10. Radiograms of a test chart using the polycapillary according to changes in the height.

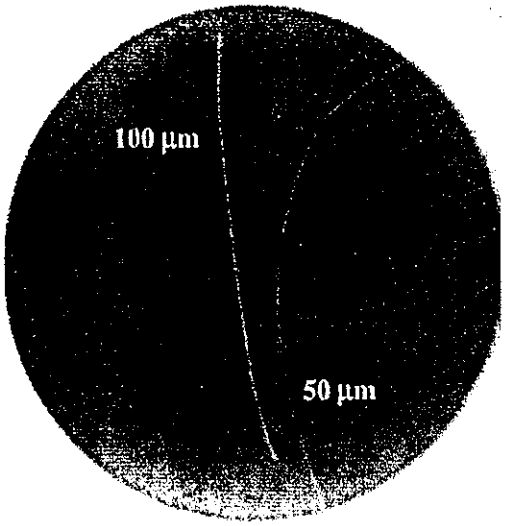

Fig. 12. Radiograms of tungsten wires on a PMMA spacer.

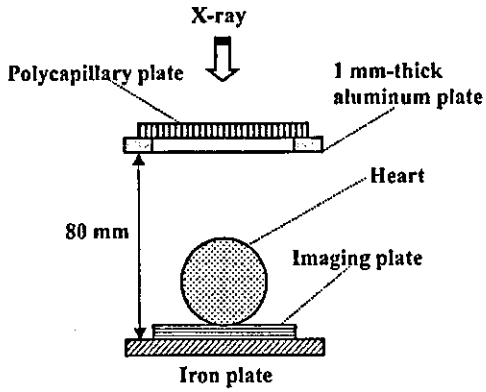

Fig. 13. Parallel angiography of a heart extracted from a rabbit using iodine-based microspheres.

microspheres of 15 μm-diameter were used, and fine blood vessels of about 100 μm were clearly visible (Fig. 14).

5. Discussion

Using this polycapillary plate, we performed a quasi-monochromatic parallel radiography system using a polycapillary plate in conjunction with a CR system.

If we assume that the incident angle for reflection in the capillary hole is constant, the X-ray intensity without absorbing I_0, the transmission intensity I_t, the reflecting intensity I_r, and the intensity for parallel radiography I may be given by (Fig. 15):

$$I_0 = K_1 \sum_{i=1}^{n} I_k(E_i) \exp\{-\mu(E_i)a\}, \quad (1)$$

$$I_t \cong K_2 \sum_{i=1}^{n} I_k(E_i) \exp\{-\mu(E_i)a - \mu_c(E_i)b\}, \quad (2)$$

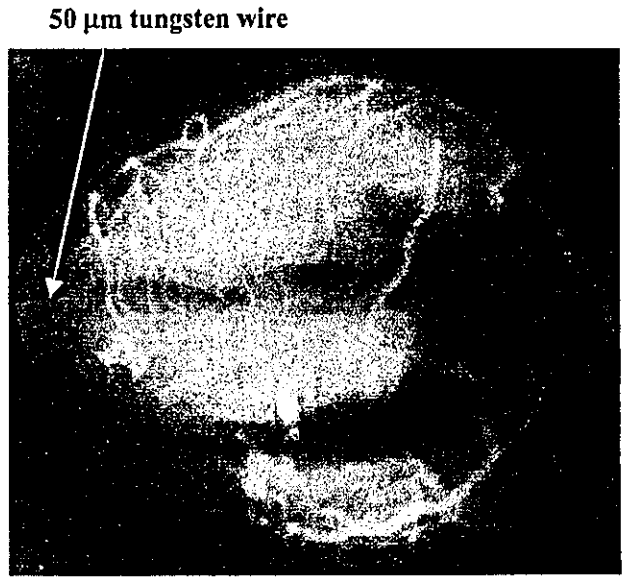

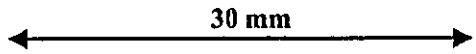

Fig. 14. Angiogram of the heart using the polycapillary.

$$I_r \cong K_3 \sum_{i=1}^{n} I_k(E_i) \exp\{-\mu(E_i)a\} \cdot R(E_i)^m, \quad (3)$$

$$I \cong I_0 + I_r \gg I_t, \quad (4)$$

where $I_k(E_i)$ is the ith characteristic X-ray intensity from the tube, $\mu(E_i)$ the linear absorption coefficient of copper filter, $\mu_c(E_i)$ is the linear absorption coefficient of capillary glass, $R(E_i)$ is the reflecting power ($1 \geqq R(E_i) \geqq 0$), m is the number of reflection, n is the number of characteristic X-rays, a is the filter thickness, b is capillary thickness, and K_1–K_3 are constants.

In this research, we performed parallel radiography achieved with a polycapillary plate in conjunction with quasi-monochromatic X-rays, and higher image resolutions as compared with those obtained without using the plate were obtained. Currently, because the resolution improves

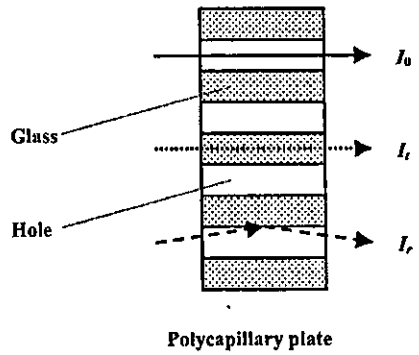

Fig. 15. Characteristic X-ray transmissions in the polycapillary plate. In the parallel radiography, the radiographic object is taken by both the direct transmission rays through capillaries I_0 and the reflection rays on the insides of holes I_r.

with corresponding decreases in the hole diameter of the capillary, this system can be applied to image a wide variety of objects in various fields including medical radiography.

6. Summary

In summary, we developed a conventional quasi-monochromatic parallel radiography system utilizing a polycapillary plate with a hole diameter of 25 μm and a CR system. Quasi-monochromatic characteristic X-rays were obtained by a 10 μm-thick copper filter with a tube voltage of 20 kV. The X-rays from the tube were formed into parallel beams in order to perform radiography. The image dimension increased slightly with corresponding increases in the distance between the radiographic object and the imaging plate, and we observed a 50 μm tungsten wire and fine blood vessels clearly.

Acknowledgements

This work was supported by Grants-in-Aid for Scientific Research and Advanced Medical Scientific Research from MECSST (12670902, 13470154, and 13877114), Grants from Keiryo Research Foundation, JST (Test of Fostering Potential), NEDO, and MHLW (HLSRG, RAMT-nano-001, RHGTEFB-genome-005, and RGCD13C-1).

References

[1] E. Sato, S. Kimura, S. Kawasaki, H. Isobe, K. Takahashi, Y. Tamakawa, T. Yanagisawa, Rev. Sci. Instrum. 61 (1990) 2343.
[2] E. Sato, A. Shikoda, S. Kimura, M. Sagae, T. Oizumi, K. Takahashi, Y. Hayasi, T. Shoji, K. Shishido, Y. Tamakawa, T. Yanagisawa, SPIE 1801 (1992) 628.
[3] E. Sato, M. Sagae, K. Takahashi, T. Oizumi, H. Ojima, K. Takayama, Y. Tamakawa, T. Yanagisawa, A. Fujiwara, K. Mitoya, SPIE 2513 (1994) 649.
[4] E. Sato, M. Sagae, K. Takahashi, A. Shikoda, T. Oizumi, H. Ojima, K. Takayama, Y. Tamakawa, T. Yanagisawa, A. Fujiwara, K. Mitoya, SPIE 2513 (1994) 723.
[5] A. Shikoda, E. Sato, M. Sagae, T. Oizumi, Y. Tamakawa, T. Yanagisawa, Rev. Sci. Instrum. 65 (1994) 850.
[6] E. Sato, K. Takahashi, M. Sagae, S. Kimura, T. Oizumi, Y. Hayasi, Y. Tamakawa, T. Yanagisawa, Med. Biol. Eng. Comput. 32 (1994) 289.
[7] K. Takahashi, E. Sato, M. Sagae, T. Oizumi, Y. Tamakawa, T. Yanagisawa, Jpn. J. Appl. Phys. 33 (1994) 4146.
[8] E. Sato, M. Sagae, A. Shikoda, K. Takahashi, T. Oizumi, M. Yamamoto, A. Takabe, K. Sakamaki, Y. Hayasi, H. Ojima, K. Takayama, Y. Tamakawa, SPIE 2869 (1996) 937.
[9] E. Sato, R. Germer, Y. Hayasi, E. Tanaka, H. Mori, T. Kawai, T. Usuki, K. Sato, H. Obara, M. Zuguchi, T. Ichimaru, H. Ojima, K. Takayama, H. Ido, SPIE 4948 (2002) 604.
[10] E. Sato, Y. Hayasi, R. Germer, E. Tanaka, H. Mori, T. Kawai, H. Obara, T. Ichimaru, K. Takayama, H. Ido, Jpn. J. Med. Imag. Inform. Sci. 20 (2003) 148.
[11] E. Sato, Y. Hayasi, R. Germer, E. Tanaka, H. Mori, T. Kawai, H. Obara, T. Ichimaru, K. Takayama, H. Ido, Jpn. J. Med. Phys. 20 (2003) 123.
[12] H. Mori, K. Hyodo, E. Tanaka, M.U. Mohammed, A. Yamakawa, Y. Shinozaki, H. Nakazawa, Y. Tanaka, T. Sekka, Y. Iwata, S. Honda, K. Umetani, H. Ueki, T. Yokoyama, K. Tanioka, M. Kubota, H. Hosaka, N. Ishizawa, M. Ando, Radiology 201 (1996) 173.
[13] T.J. Davis, D. Gao, T.E. Gureyev, A.W. Stevenson, S.W. Wilkins, Nature 373 (1995) 595.
[14] A. Momose, T. Takeda, Y. Itai, K. Hirano, Nat. Med. 2 (4) (1996) 473.
[15] A. Ishisaka, H. Ohara, C. Honda, Opt. Rev. 7 (2000) 566.
[16] A.A. Bzhanmikov, N. Langhoff, J. Schmalz, R. Wedell, V.L. Beloglazov, N.F. Lebedev, SPIE 3444 (1998) 430.
[17] Q.F. Xiao, S.V. Poturaef, Nucl. Instr. Meth. Phys. Res. A 347 (1994) 376.
[18] E. Sato, Y. Hayasi, E. Tanaka, H. Mori, T. Kawai, H. Obara, T. Ichimaru, K. Takayama, H. Ido, T. Usuki, K. Sato, Y. Tamakawa, SPIE 4508 (2001) 176.
[19] E. Sato, H. Toriyabe, Y. Hayasi, E. Tanaka, H. Mori, T. Kawai, T. Usuki, K. Sato, H. Obara, T. Ichimaru, K. Takayama, H. Ido, Y. Tamakawa, SPIE 4682 (2002) 298.
[20] E. Sato, Y. Hayasi, T. Usuki, K. Sato, H. Ojima, K. Takayama, H. Ido, in: Proceedings of the 3rd Korea-Japan Joint Meeting on Medical Physics, Gyeongju, 2002, p. 400.
[21] E. Sato, K. Sato, Y. Tamakawa, Ann. Rep. Iwate Med. Univ. Sch. Lib. Arts Sci. 35 (2000) 13.

Available online at www.sciencedirect.com
SCIENCE DIRECT®
JOURNAL OF ELECTRON SPECTROSCOPY and Related Phenomena
ELSEVIER
Journal of Electron Spectroscopy and Related Phenomena 137–140 (2004) 713–720
www.elsevier.com/locate/elspec

Sharp characteristic X-ray irradiation from weakly ionized linear plasma

E. Sato[a,*], Y. Hayasi[a], R. Germer[b], E. Tanaka[c], H. Mori[d], T. Kawai[e], T. Ichimaru[f], S. Sato[g], K. Takayama[h], H. Ido[i]

[a] *Department of Physics, Iwate Medical University, Morioka 020-0015, Japan*
[b] *ITP, FHTW FB1 and TU-Berlin, D 12249 Berlin, Germany*
[c] *Department of Nutritional Science, Faculty of Applied Bio-science, Tokyo University of Agriculture, Setagayaku 156-8502, Japan*
[d] *Department of Cardiac Physiology, National Cardiovascular Center Research Institute, Osaka 565-8565, Japan*
[e] *Electron Tube Division #2, Hamamatsu Photonics Inc., Iwata-gun 438-0193, Japan*
[f] *Department of Radiological Technology, School of Health Sciences, Hirosaki University, Hirosaki 036-8564, Japan*
[g] *Department of Microbiology, School of Medicine, Iwate Medical University, Morioka 020-8505, Japan*
[h] *Shock Wave Research Center, Institute of Fluid Science, Tohoku University, Sendai 980-8577, Japan*
[i] *Department of Applied Physics and Informatics, Faculty of Engineering, Tohoku Gakuin University, Tagajo 985-8537, Japan*

Available online 21 March 2004

Abstract

In the plasma flash X-ray generator, a high-voltage main condenser of approximately 200 nF is charged up to 50 kV by a power supply, and electric charges in the condenser are discharged to an X-ray tube after triggering the cathode electrode. Flash X-rays are then produced. The X-ray tube is a demountable triode connected to a turbo molecular pump with a pressure of approximately 1 mPa. As electrons from the cathode electrode are roughly focused onto a rod nickel target of 3.0 mm in diameter by the electric field in the X-ray tube, a weakly ionized linear plasma consisting of nickel ions and electrons forms by target evaporation. At a charging voltage of 50 kV, the maximum tube voltage was almost equal to the charging voltage of the main condenser, and the peak current was about 17 kA. When the charging voltage was increased, the linear plasma formed, and the intensities of K-series characteristic X-rays increased. The K-series lines were quite sharp and intense, and hardly any bremsstrahlung rays were detected. The X-ray pulse widths were approximately 700 ns, and the time-integrated X-ray intensity had a value of approximately 30 μC/kg at 1.0 m from the X-ray source at a charging voltage of 50 kV.

Keywords: Flash X-ray; Weakly ionized linear plasma; K-series characteristic X-rays; Quasi-monochromatic X-rays; Monochromatic X-rays

1. Introduction

Flash X-ray generators utilizing condensers are of great technological importance due to their extremely short X-ray durations, and several different types of generators have been developed for specific radiographic applications [1,2]. In particular, flash X-ray generators with energies lower than 150 keV have been developed in order to perform soft radiographies with biomedical applications [3–8], and these generators have large capacity condensers in order to increase the X-ray intensity by increasing electrostatic energy.

Using a gas-discharge capillary [9–12], soft X-ray lasers have been produced to form a linear plasma, in which the laser intensity increases proportionally to the capillary length. However, it is quite difficult to increase the laser photon energy beyond 10 keV. Because there are no X-ray resonators in the high photon energy region, new methods for increasing coherence will be desired in the future.

By forming a weakly ionized linear plasma [13–16] using plate and rod targets, we confirmed the production of intense K-series characteristic X-rays along the plasma axial direction. In these experiments, because we employed a transmission-type X-ray spectrometer utilizing an X-ray film, it was difficult to determine the relative intensities of the characteristic X-rays.

In this paper, we describe a flash X-ray generator utilizing a large capacity condenser of 200 nF and a rod-target

* Corresponding author.
E-mail address: dresato@iwate-med.ac.jp (E. Sato).

0368-2048/$ – see front matter © 2004 Elsevier B.V. All rights reserved.
doi:10.1016/j.elspec.2004.02.009

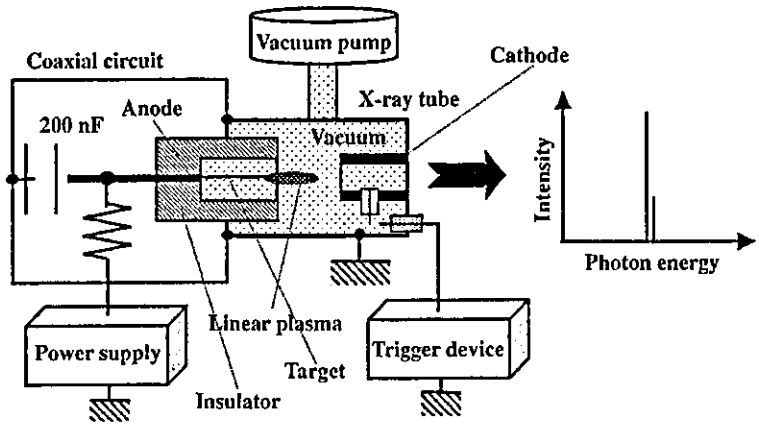

Fig. 1. Block diagram of the high-intensity plasma flash X-ray generator. This generator employs a large capacity condenser in order to increase the characteristic X-ray intensities in a low photon energy region by increasing the electrostatic energy in the condenser.

radiation tube, used to perform a preliminary experiment for generating intense and sharp monochromatic X-rays by forming a linear nickel plasma cloud around a fine target.

2. Generator

2.1. High-voltage circuit

Fig. 1 shows a block diagram of the high-intensity plasma flash X-ray generator. This generator consists of the following essential components: a high-voltage power supply, a high-voltage condenser with a capacity of approximately 200 nF, a turbo-molecular vacuum pump, a krytron pulse generator as a trigger device, and a flash X-ray tube. In this generator, a low-impedance transmission line is employed in order to increase maximum tube current. The high-voltage main condenser is charged to 50 kV by the power supply, and electric charges in the condenser are discharged to the tube after triggering the cathode electrode. The plasma flash X-rays are then produced.

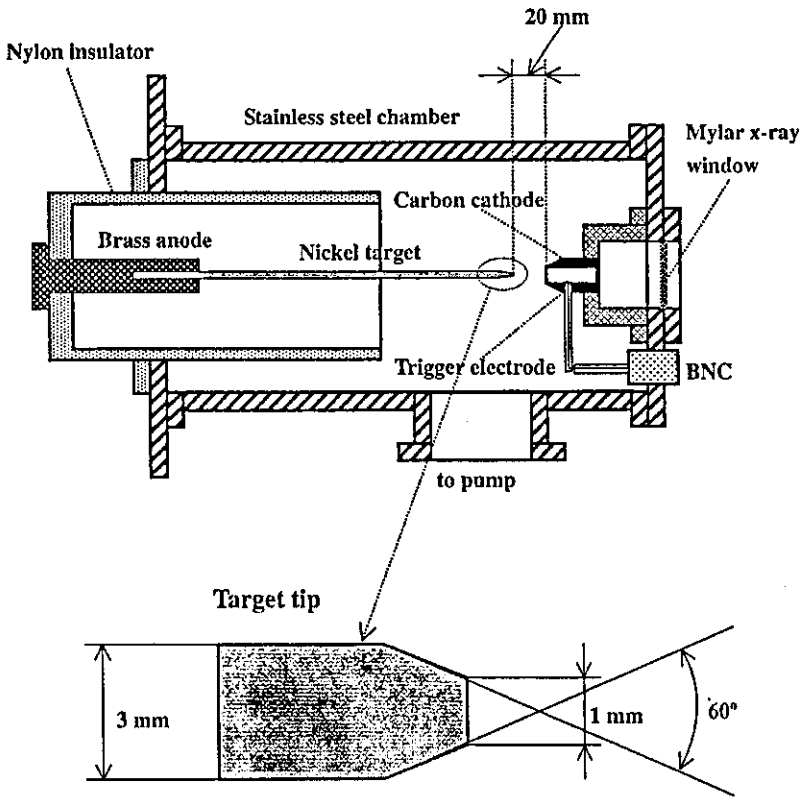

Fig. 2. Schematic drawing of the flash X-ray tube with a rod target. The tube utilizes a long target to form a weakly ionized linear plasma to absorb bremsstrahlung X-rays produced in the plasma, which transmits the characteristic X-rays easily due to the absorption coefficient.

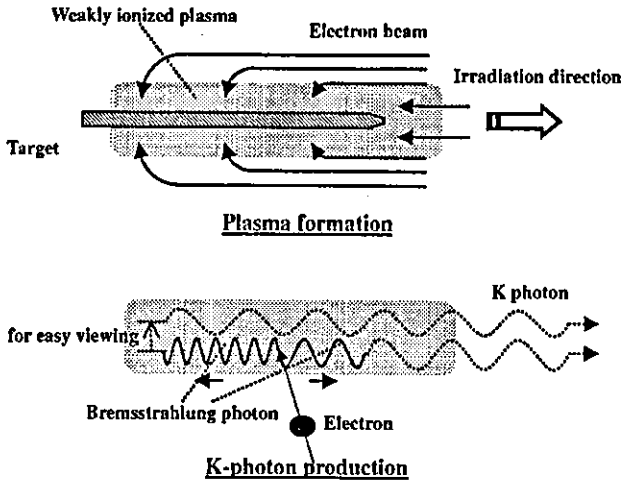

Fig. 3. K-photon irradiation from the plasma. The bremsstrahlung X-rays are absorbed and are converted into fluorescent (characteristic) X-rays in the weakly ionized linear plasma.

2.2. X-ray tube

The X-ray tube is a demountable cold cathode triode connected to a turbo-molecular pump. The pressure in the tube is approximately 1 mPa (Fig. 2). The tube consists of the following major parts: a hollow cylindrical carbon cathode with a bore diameter of 10.0 mm, a trigger electrode made from copper wire, a stainless steel vacuum chamber, a nylon insulator, a polyethylene terephthalate (Mylar) X-ray window 0.25 mm in thickness, and a rod-shaped nickel target 3.0 mm in diameter with a tip angle of 60°. The distance between the target and cathode electrodes is approximately 20 mm, and the trigger electrode is set in the cathode electrode. The electron beam from the cathode electrode is roughly focused onto the target by the electric field in the tube, and evaporation leads to the formation of a weakly ionized linear plasma of nickel ions and electrons around the fine target.

2.3. Principle of characteristic X-ray irradiation

In the linear plasma, bremsstrahlung photons with energies higher than the K-absorption edge are effectively absorbed and are converted into fluorescent X-rays (Fig. 3). The plasma then transmits the fluorescent rays easily, and bremsstrahlung rays with energies lower than the K-edge are also absorbed by the plasma. In addition, because bremsstrahlung rays are not emitted in the direction opposite that of electron acceleration, intense characteristic X-rays are generated along axial direction of the plasma.

3. Characteristics

3.1. Tube voltage and current

The tube voltage and current were measured by a high-voltage divider with an input impedance of 1 GΩ and a current transformer, respectively. Fig. 4 shows the time relation for the tube voltage and current. At the indicated charging voltages, they displayed damped oscillations. When the charging voltage was increased, both the maximum tube voltage and current increased. At a charging voltage of 50 kV, the maximum tube voltage was almost equal to the charging voltage of the main condenser, and the maximum tube current was approximately 17 kA.

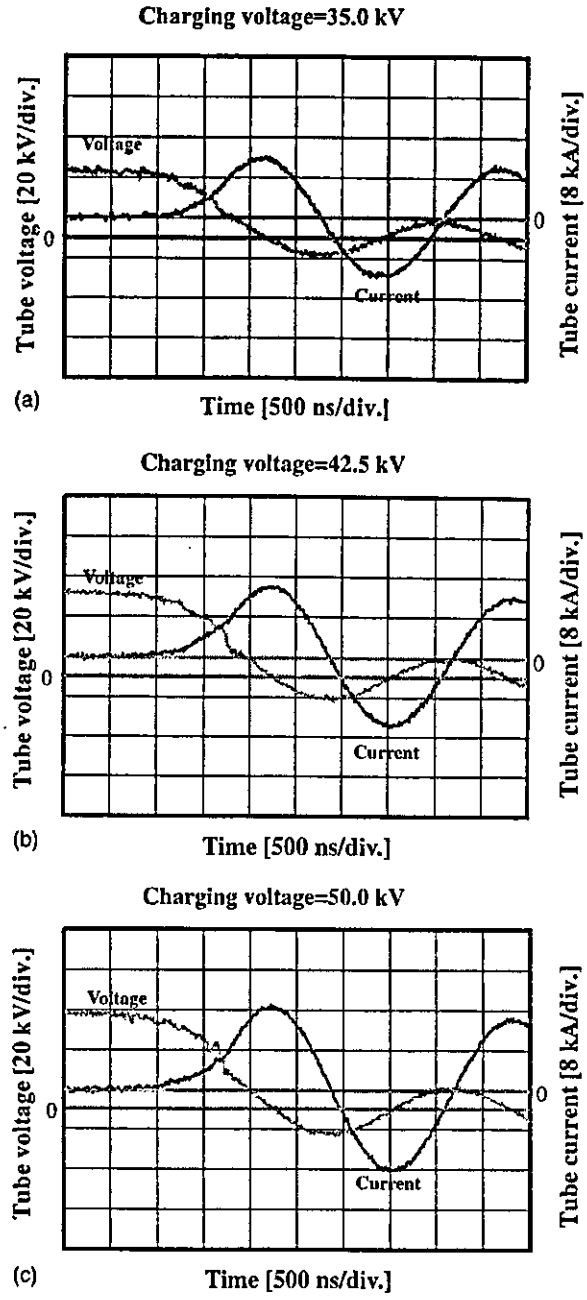

Fig. 4. Tube voltages and currents with a charging voltage of (a) 35.0, (b) 42.5, and (c) 50.0 kV.

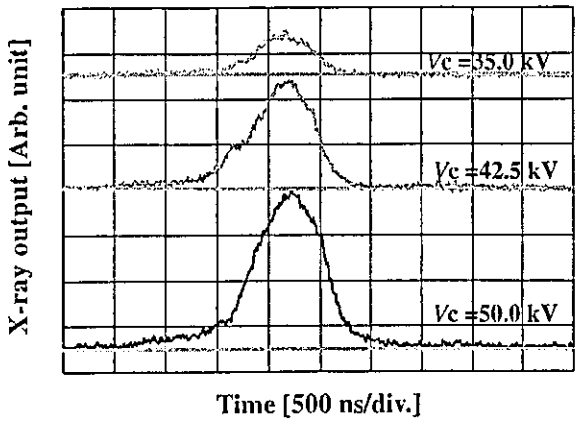

Fig. 5. X-ray outputs measured by a plastic scintillator with changes in the charging voltage.

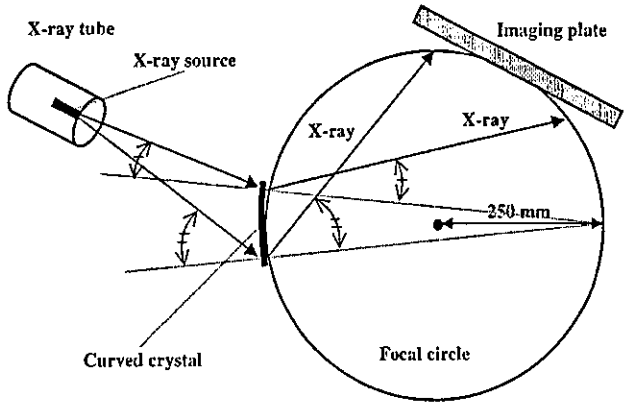

Fig. 7. Transmission-type spectrometer with a lithium fluoride curved crystal and an imaging plate. The X-rays from the source are diffracted by the crystal and are imaged by the imaging plate.

3.2. X-ray output

X-ray output pulse was detected using a combination of a plastic scintillator and a photomultiplier (Fig. 5). The X-ray pulse height substantially increased with corresponding increases in the charging voltage. The X-ray pulse widths were about 700 ns, and the time-integrated X-ray intensity per pulse, measured by a thermoluminescence dosimeter (Kyokko TLD Reader 1500 having MSO-S elements without energy compensation), had a value of about 30 μC/kg at 1.0 m from the X-ray source with a charging voltage of 50 kV.

3.3. X-ray source

The images of the plasma X-ray source were taken using a pinhole camera with a hole diameter of 100 μm (Fig. 6). When the charging voltage was increased, the plasma X-ray source grew, and both the beam dimension and the intensity increased.

3.4. X-ray spectra

X-ray spectra from the plasma source were measured by a transmission-type spectrometer (Fig. 7) with a lithium fluoride curved crystal of 0.5 mm in thickness. The spectra were taken by a computed radiography (CR) system (Konica Regius 150) [17] with a wide dynamic range, and the relative X-ray intensity was calculated from Dicom digital data. Fig. 8 shows measured spectra from the nickel target. We observed quite sharp lines of K-series characteristic X-rays such as lasers, while bremsstrahlung rays were hardly detected. The characteristic X-ray intensities of K_α and K_β lines substantially increased with corresponding increases in the charging voltage, and the K_β line was absorbed by a monochromatic cobalt filter of 15 μm thickness.

3.5. X-ray divergence

In order to ascertain the difference in characteristics between X-rays from a conventional tube and these from the

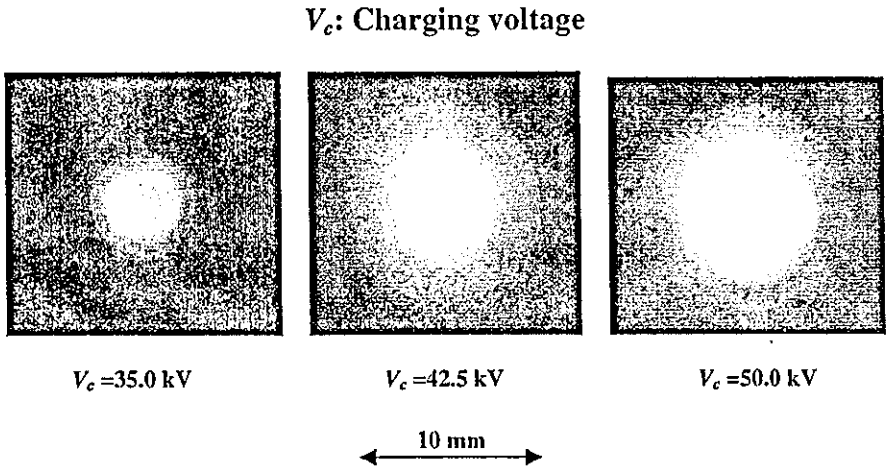

Fig. 6. Images of the plasma X-ray source measured by a pinhole of 100 μm from the plasma axial direction.

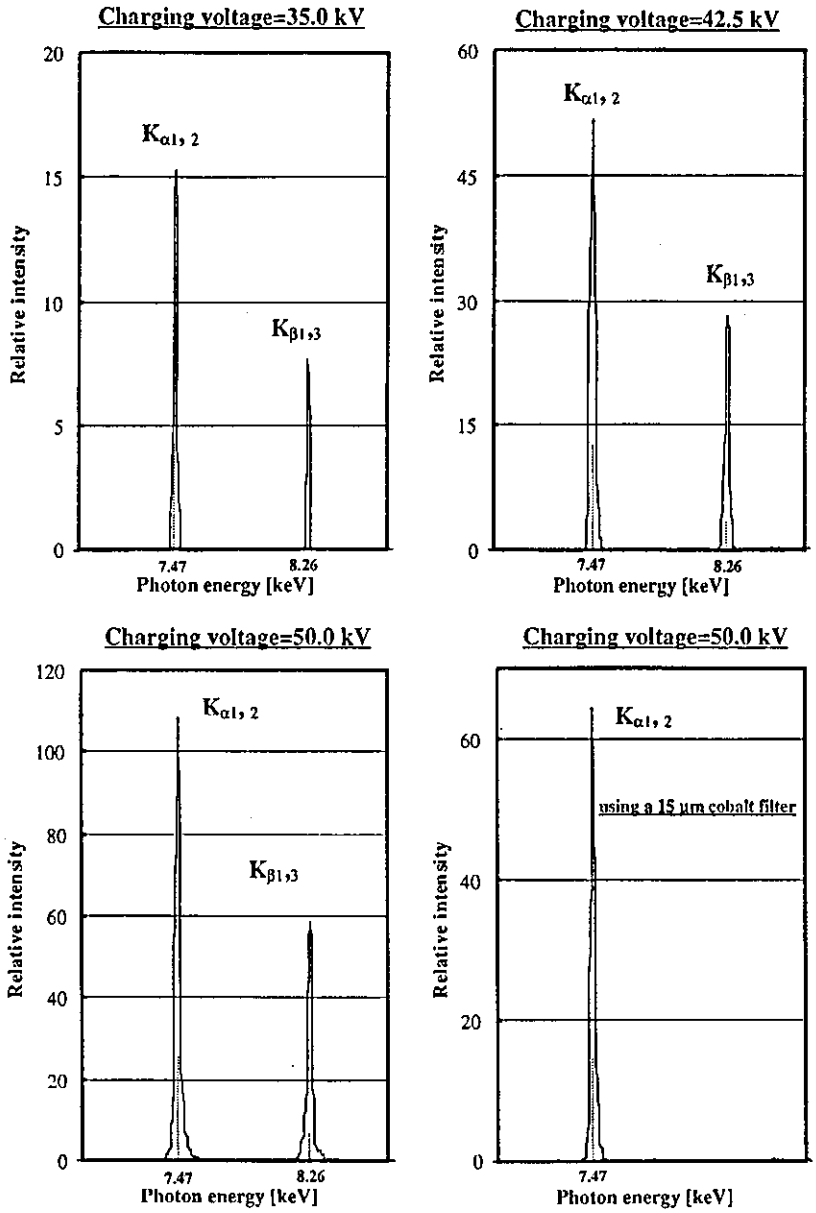

Fig. 8. X-ray spectra from weakly ionized nickel plasma according to changes in the charging voltage and to insertion of a cobalt monochromatic filter. In the measurement, we observed very sharp and intense characteristic X-rays such as lasers, while bremsstrahlung X-rays were hardly detected at all.

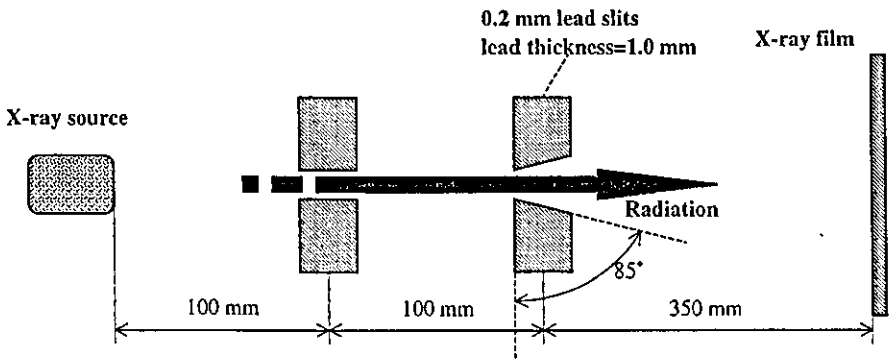

Fig. 9. Experimental setup for measuring X-ray divergence using two lead slits.

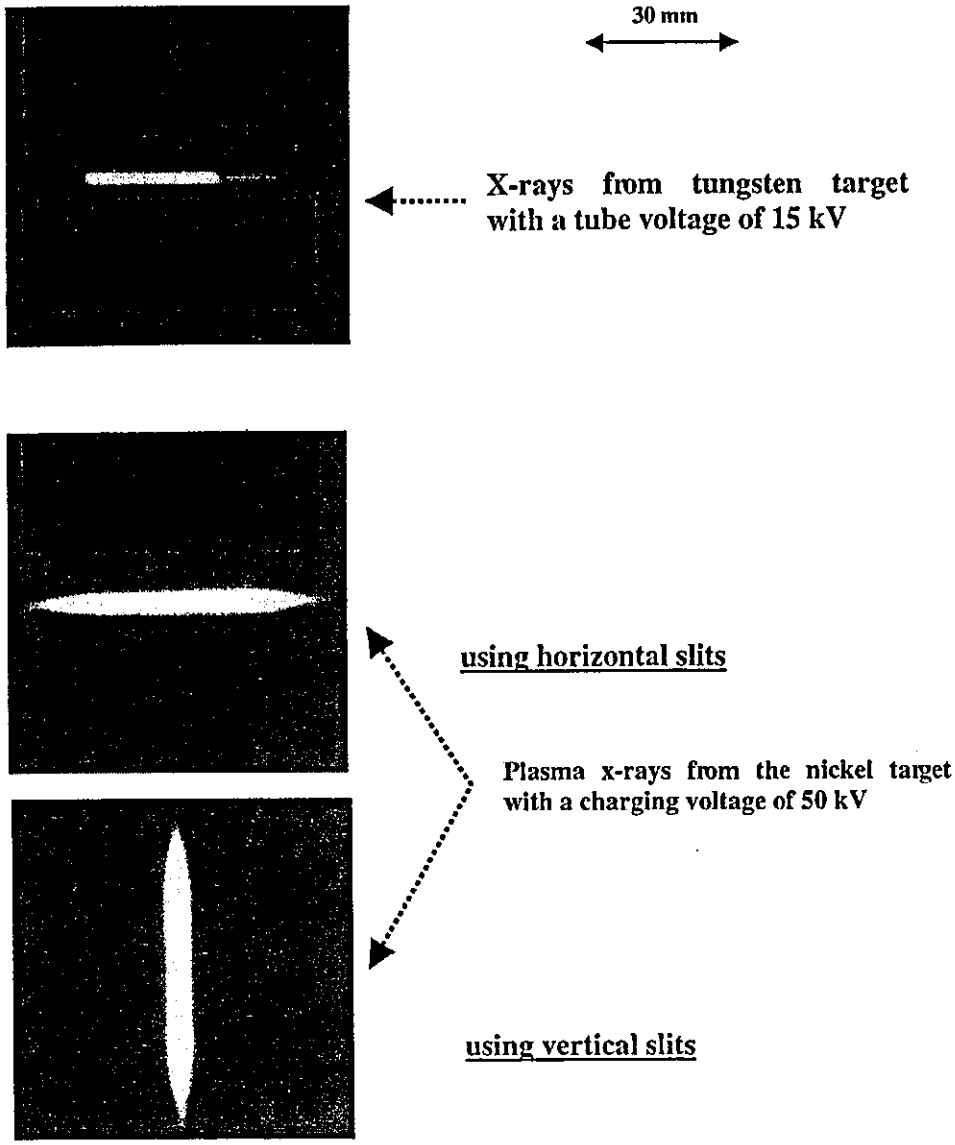

Fig. 10. X-ray divergence with two lead slits. The characteristic X-rays from the plasma were diffused greatly after passing through two lead slits.

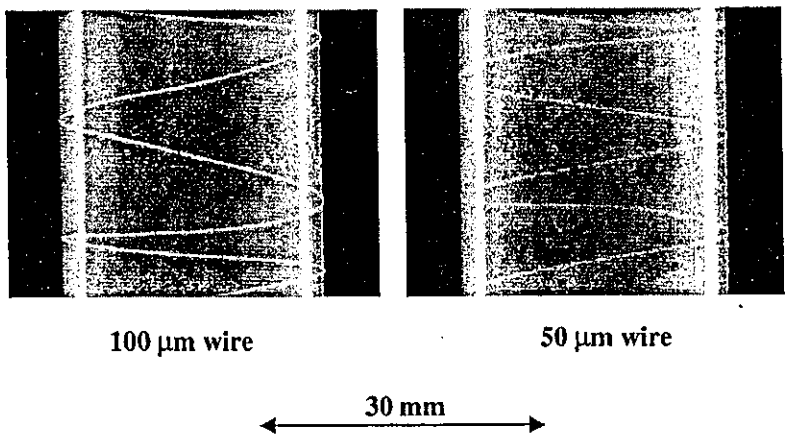

Fig. 11. Radiograms of tungsten wires of 50 and 100 μm in diameter coiled around pipes made of polymethyl methacrylate.

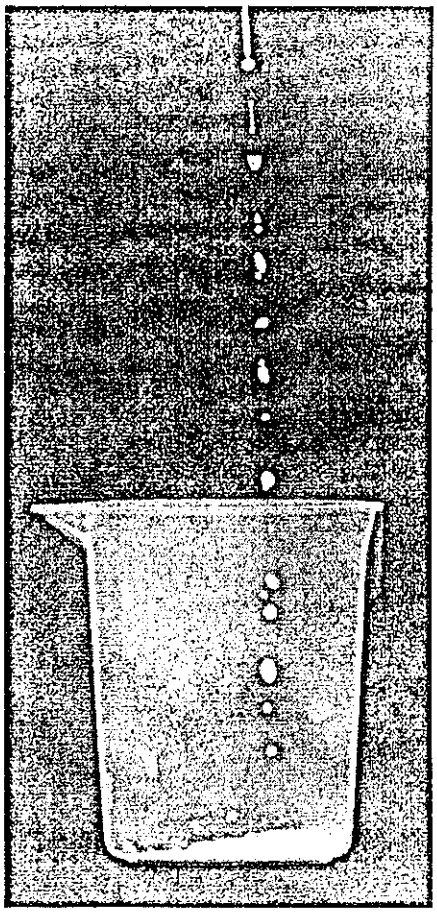

Fig. 12. Radiogram of water droplets falling into a polypropylene beaker from an injector.

plasma tube, we employed two lead slits in order to measure the divergence of the X-rays (Fig. 9). As compared with X-rays from a conventional tube with a tungsten target, the characteristic X-rays from the linear plasma were diffused greatly after passing through the two slits (Fig. 10).

4. Radiography

The plasma radiography was performed by the CR system (Konica Regius 150) without using a monochromatic filter, and the distance between the X-ray source and imaging plate was 1.2 m.

Firstly, the image resolution was measured using wires. Fig. 11 shows radiograms of tungsten wires coiled around pipes made of polymethyl methacrylate at a charging voltage of 50 kV. Although the image contrast increased with increases in the wire diameter, a 50 μm-diameter wire could be observed.

The image of water droplets falling into a polypropylene beaker from an injector is shown in Fig. 12. This image

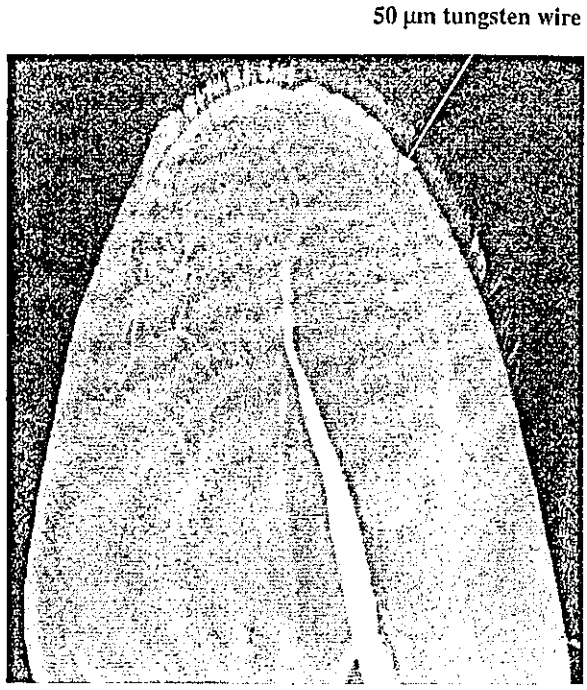

Fig. 13. Angiograms of the external ear of a rabbit.

was taken at a charging voltage of 45 kV, with the slight addition of an iodine-based contrast medium. Because the X-ray duration was about 1 μs, the stop-motion image of water could be obtained.

Fig. 13 shows an angiogram of the external ear of a rabbit; iodine-based microspheres of 15 μm diameter were used at a charging voltage of 45 kV, and fine blood vessels of about 50 μm were clearly visible.

5. Discussion

Regarding the spectrum measurement, although we obtained quite intense and sharp K-series lines without bremsstrahlung X-rays by forming a linear plasma X-ray source, we could not observe the difference between the $K\alpha_1$ and $K\alpha_2$ lines. In addition, we confirmed the divergence of K-series characteristic X-rays using two lead slits, and the maximum divergence angle was approximately 0.5°.

If we assume that the characteristic and bremsstrahlung X-rays are signal and noise, respectively, the signal to noise ratio is higher than 1000:1, and this value is almost equal to those of soft X-ray lasers produced by the gas-discharge capillary.

In this research, we obtained sufficient characteristic X-ray intensity per pulse for CR radiography, and the generator produced number of characteristic photons of approximately 1×10^{14} photons/cm^2 s at 1.0 m from the source. In addition, since the photon energy of characteristic X-rays can be controlled by changing target elements, various quasi-monochromatic high-speed radiographies,

such as high-contrast micro angiography[22] and parallel radiography[23] using an X-ray lens, will be possible.

Acknowledgements

This work was supported by Grants-in-Aid for Scientific Research and Advanced Medical Scientific Research from MECSST (12670902, 13470154, and 13877114), Grants from Keiryo Research Foundation, JST (Test of Fostering Potential), NEDO, and MHLW (HLSRG, RAMT-nano-001, RHGTEFB-genome-005, and RGCD13C-1).

References

[1] A. Mattsson, Physica Scripta 5 (1972) 99.
[2] R. Germer, J. Phys. E: Sci. Instrum. 12 (1979) 336.
[3] E. Sato, H. Isobe, F. Hoshino, Rev. Sci. Instrum 57 (1986) 1399.
[4] E. Sato, S. Kimura, S. Kawasaki, H. Isobe, K. Takahashi, Y. Tamakawa, T. Yanagisawa, Rev. Sci. Instrum. 61 (1990) 2343.
[5] A. Shikoda, E. Sato, M. Sagae, T. Oizumi, Y. Tamakawa, T. Yanagisawa, Rev. Sci. Instrum. 65 (1994) 850.
[6] E. Sato, K. Takahashi, M. Sagae, S. Kimura, T. Oizumi, Y. Hayasi, Y. Tamakawa, T. Yanagisawa, Med. Biol. Eng. Comput. 32 (1994) 289.
[7] K. Takahashi, E. Sato, M. Sagae, T. Oizumi, Y. Tamakawa, T. Yanagisawa, Jpn. J. Appl. Phys. 33 (1994) 4146.
[8] E. Sato, M. Sagae, A. Shikoda, K. Takahashi, T. Oizumi, M. Yamamoto, A. Takabe, K. Sakamaki, Y. Hayasi, H. Ojima, K. Takayama, Y. Tamakawa, SPIE 2869 (1996) 937.
[9] J.J. Rocca, V. Shlyaptsev, F.G. Tomasel, Phys. Rev. Lett. 73 (1994) 2192.
[10] G.P. Collins, Phys. Today 10 (1994) 19.
[11] J.J.G. Rocca, J.L.A. Chilla, S. Sakadzic, SPIE 4505 (2001) 1.
[12] S. Le Pape, P. Zeitoun, J.J.G. Rocca, SPIE 4505 (2001) 23.
[13] E. Sato, Y. Suzuki, Y. Hayasi, E. Tanaka, H. Mori, T. Kawai, K. Takayama, H. Ido, Y. Tamakawa, SPIE 4505 (2001) 154.
[14] E. Sato, Y. Hayashi, E. Tanaka, H. Mori, T. Kawai, H. Obara, T. Ichimaru, K. Takayama, H. Ido, T. Usuki, K. Sato, Y. Tamakawa, SPIE 4508 (2001) 176.
[15] E. Sato, Y. Hayasi, R. Germer, E. Tanaka, H. Mori, T. Kawai, H. Obara, T. Ichimaru, K. Takayama, H. Ido, Jpn. J. Med. Imag. Inform. Sci. 20 (2003) 148.
[16] E. Sato, Y. Hayasi, R. Germer, E. Tanaka, H. Mori, T. Kawai, H. Obara, T. Ichimaru, K. Takayama, H. Ido, Jpn. J. Med. Phys. 20 (2003) 123.
[17] E. Sato, K. Sato, Y. Tamakawa, Ann. Rep. Iwate Med. Univ. Sch. Lib. Arts Sci. 35 (2000) 13.

In Situ Measurements of Crossbridge Dynamics and Lattice Spacing in Rat Hearts by X-Ray Diffraction

Sensitivity to Regional Ischemia

James T. Pearson, PhD; Mikiyasu Shirai, MD, PhD; Haruo Ito, PhD; Noriyuki Tokunaga, MD; Hirotsugu Tsuchimochi, PhD; Naoki Nishiura; Daryl O. Schwenke, PhD; Hatsue Ishibashi-Ueda, MD; Ryuichi Akiyama, PhD; Hidezo Mori, MD, PhD; Kenji Kangawa, PhD; Hiroyuki Suga, MD, PhD; Naoto Yagi, PhD

Background—Synchrotron radiation has been used to analyze crossbridge dynamics in isolated papillary muscle and excised perfused hearts with the use of x-ray diffraction techniques. We showed that these techniques can detect regional changes in rat left ventricle contractility and myosin lattice spacing in in situ ejecting hearts in real time. Furthermore, we examined the sensitivity of these indexes to regional ischemia.

Methods and Results—The left ventricular free wall of spontaneously beating rat hearts (heart rate, 290 to 404 bpm) was directly exposed to brief high-flux, low-emittance x-ray beams provided at SPring-8. Myosin mass transfer to actin filaments was determined as the decrease in reflection intensity ratio (intensity of 1,0 plane over the 1,1 plane) between end-diastole and end-systole. The distance between 1,0 reflections was converted to a lattice spacing between myosin filaments. We found that mass transfer (mean, 1.71±0.09 SEM, n=13 hearts) preceded significant increases in lattice spacing (2 to 5 nm) during systole in nonischemic pericardium. Left coronary occlusion eliminated increases in lattice spacing and severely reduced mass transfer ($P<0.01$) in the ischemic region.

Conclusions—Our results suggest that x-ray diffraction techniques permit real-time in situ analysis of regional crossbridge dynamics at molecular and fiber levels that might also facilitate investigations of ventricular output regulation by the Frank-Starling mechanism. ***(Circulation.* 2004;109:2976-2979.)**

Key Words: ischemia ■ myocardial contraction ■ myosin ■ radiography

Despite the history of studies on crossbridge dynamics, lower photon counts and poorer quality of diffraction patterns obtained from cardiac muscle than skeletal and insect flight muscles[1–3] have limited progress with cardiac muscle until recently.[4,5] Some of us used third-generation synchrotron radiation (SPring-8, Japan Synchrotron Radiation Research Institute) to determine x-ray diffraction patterns in excised, perfused rat hearts while moving systematically across the left ventricular (LV) equator from the epicardium through to the ventricular cavity.[6]

X-ray diffraction patterns of cardiac muscle produce 2 equatorial-position reflections from the lattice-like arrangement of its protein elements.[2] Mass transfer of myosin heads to actin during contraction is inferred from a decrease in the integrated 1,0 reflection intensity ($I_{1,0}$, lattice plane containing only thick myosin filaments) and an increase in 1,1 reflection intensity ($I_{1,1}$, plane with thick myosin and thin actin filaments).[7] The myocardial intensity ratio (defined as $I_{1,0}/I_{1,1}$) is minimal in the rigor state and maximal in a quiescent state.[1,2,6,8]

Furthermore, the distance between 1,0 reflection peaks ($d_{1,0}$ spacing) represents the myosin lattice spacing, which is inversely related to sarcomere length in isolated fibers[5] as static myocytes maintain a constant cell volume. Whether decreases in myofilament spacing contribute to increasing Ca^{2+} sensitivity and increased probability of crossbridge formation at longer sarcomere lengths has been actively debated.[9] However, it is still not known if lattice spacing is regulated to maintain constant lattice volume (ie, if lattice cross-sectional area decreases with increasing sarcomere length, then interfilament spacing must decrease) during dynamic contractions in vivo.

Recently, it was shown that the intensity ratio derived from x-ray diffraction patterns of isolated whole hearts decreased during isovolumic contractions with a similar time course throughout the LV,[6] implying that crossbridge cycling in fibers of different myocardial layers is similar despite differences in fiber orientation and rate of short-

Received March 1, 2004; de novo received March 31, 2004; revision received May 6, 2004; accepted May 6, 2004.

From the National Cardiovascular Center Research Institute, Osaka, Japan (J.T.P., M.S., N.T., H.T., N.N., D.O.S., H.I.-U., H.M., K.K., H.S.); S-I Medico-Tech Co Ltd, Kashiwara, Osaka, Japan (H.I.); Muroran Institute of Technology, Muroran, Japan (R.A.); and SPring-8/JASRI, Sayo, Hyogo, Japan (N.Y.)

Correspondence to Dr James T. Pearson, Cardiac Physiology, National Cardiovascular Center Research Institute, 5-7-1 Fujishirodai, Suita, Osaka 565-8565 Japan. E-mail jpearson@ri.ncvc.go.jp

Circulation is available at http://www.circulationaha.org

DOI: 10.1161/01.CIR.0000133322.19340.FF